Magnetic resonance diffusion-weighted imaging: quantitative evaluation of age-related changes in healthy liver parenchyma.

Available online at www.sciencedirect.com
ScienceDirect
Magnetic Resonance Imaging 29 (2011) 805–812
MAGNETIC RESONANCE IMAGING

Magnetic resonance diffusion-weighted imaging: quantitative evaluation of age-related changes in healthy liver parenchyma

Filippo Pasquinelli[a], Giacomo Belli[b], Lorenzo Nicola Mazzoni[c], Luigi Grazioli[d], Stefano Colagrande[a,*]

[a]*Section of Radiodiagnostics, Department of Clinical Physiopathology, University of Florence, Azienda Ospedaliero-Universitaria, 50134 Florence, Italy*
[b]*Section of Medical Physics, Azienda Ospedaliero-Universitaria Careggi, 50134 Florence, Italy*
[c]*CIRM, University of Florence, Azienda Ospedaliero-Universitaria Careggi, 50134 Florence, Italy*
[d]*Department of Radiology, Azienda Ospedaliera Spedali Civili Brescia, 25123 Brescia, Italy*

Received 1 July 2010; revised 4 November 2010; accepted 20 February 2011

Abstract

The purpose of this study was to verify in healthy liver parenchyma the possible influence of age on DwI-related parameters: apparent diffusion coefficient (ADC), perfusion fraction (PF), diffusion and pseudodiffusion coefficient (*D* and *D**). Forty healthy adult volunteers (age range 26–86 years), divided into four age groups, were prospectively submitted to a breath-hold magnetic resonance diffusion imaging (MR-DwI) (two *b* values, 0–300 and 0–1000 s/mm^2). A smaller cohort of 16 subjects underwent a free-breath multi-*b* acquisition (16 *b* values, 0–750 s/mm^2). Quantitative analysis was performed by two observers with manually defined regions of interest, on the most homogeneous portion of the right liver lobe. Individual and group statistical analysis of data was performed: ANOVA to establish differences between groups and Pearson correlation coefficient to investigate the association between DwI parameters and age. The mean, S.D. and 95% limits of agreement of ADC values for each age-defined group are reported. ANOVA showed no significant differences between group means (*P* always >.05). No significant correlation between subjects' age and DwI parameters was established, both in breath-hold and free-breath acquisitions, on the whole range of adopted *b* values. Our study conducted on healthy liver parenchyma shows that there are no significant differences in ADC, PF, *D* and *D** of younger or older subjects.

Keywords: Aging; Apparent diffusion coefficient; Perfusion fraction; Pseudodiffusion; DwI

1. Introduction

Measurement of the apparent diffusion coefficient (ADC) by means of diffusion-weighted magnetic resonance imaging (MR-DwI) allows quantification of the combined effects of molecular Brownian motion of water within tissues and perfusion [1,2]. MR-DwI has become a tool for intensive clinical research which can quantitatively differentiate benign from malignant focal hepatic lesions or stage hepatic fibrosis [3–8]. However, the quantitative results in this field are still controversial due to several technical and physiological factors that concurrently affect ADC measurements such as *b* factor, echo time (TE), site and size of sampling methods, temperature, nondiffusional intravoxel incoherent motion (IVIM) related to perfusion, modality of acquisition (breath-hold BH, free-breath FB, echo-navigator), without considering difficulties related to intrinsic sensitivity to motion and magnetic susceptibility of Dw sequences [2,9–20].

Another physiological effect which has never been investigated, as far as we know, that could determine ADC variation in the liver is the subject's age, whose influence on quantitative DwI is still unknown [6,7].

With this background, the aim of our study was to analyze the possible influence of age on DwI main quantitative parameters, which are ADC, perfusion fraction (PF), diffusion (*D*) and pseudodiffusion (*D**).

* Corresponding author. Department of Clinical Physiopathology, Section of Radiodiagnostics, University of Florence, Azienda Ospedaliero-Universitaria Careggi, 50134 Florence, Italy. Tel.: +39 055 4377673; fax: +39 055 431970.
E-mail address: stefano.colagrande@unifi.it (S. Colagrande).

0730-725X/$ – see front matter © 2011 Elsevier Inc. All rights reserved.
doi:10.1016/j.mri.2011.02.014

2. Methods

2.1. Study participants

Forty healthy adult volunteers prospectively underwent abdominal MR-DwI from November 2009 to October 2010 (27 males, 13 females, ranging in age from 26 to 86 years, mean age 48 years). Subjects were selected to homogeneously cover the whole age range and were divided into four groups of 10 subjects each in the following age ranges: 18–30, 31–45, 46–65, >65 years, respectively, identified as Groups A, B, C, and D.

The inclusion criteria for this study were as follows: no history of illegal drug use or alcohol abuse, normal liver on ultrasound study (no focal or diffuse liver disease, including mild steatosis) [21], normal liver function tests and no history of abdominal surgery. The study protocol was approved by the investigation and ethics committee of our institution. The aim and nature of this prospective study were explained to the volunteers, each of whom provided written consent before beginning the examination, in accordance with the principles of the Declaration of Helsinki (revision of Edinburgh, 2000). All examinations were performed after overnight fasting.

2.2. In vitro MR imaging

All examinations were carried out using a 1.5-T MR body scanner (Gyroscan NT Intera Release 12, Philips, Eindhoven, The Netherlands; maximum gradient strength 30 mT/m, peak slew rate 120 mT/m/ms) equipped with a four-channel receiver coil, positioned to cover the upper abdomen of the subject lying in a supine position; the arms were extended over the head to reduce artefacts. As recommended [19], we checked the accuracy of our scanner by doing an MR-DwI phantom study [20], applying two different DwI multi-*b* acquisition sequences: the first with the sensitizing factor varied within a short range of *b* values (*b*=0–200 s/mm^2 with steps of 20 s/mm^2). This sequence enabled us to assess the gradient accuracy and the errors induced on the effective *b* value by the imaging gradients. The second sequence applied differed by a greater *b* value interval (*b*=0–1000 s/mm^2 with steps of 100 s/mm^2), and provided information on reproducibility and signal stability [20].

2.3. In vivo MR imaging

In vivo, we applied the following protocol of acquisitions on all the 40 subjects:

Axial and coronal T2-weighted half-Fourier single-shot turbo spin-echo (HASTE) free-breath sequence, TR/TE=810/80 ms, echo-train length=69, slice thickness/number=5 mm/40, intersection slice gap=10%, field of view (FOV)=300–420 mm, reconstruction matrix size=256×165, number signal averages (NSA)=1, acquisition time=2–3 min;

Axial T1-weighted 2D gradient echo in/out phase breath-hold sequence, TR/TE=231–121/14.6–2.3 ms, slice thickness/number=5 mm/ 24, intersection slice gap=10%, flip angle=80, sense factor 1.5, FOV=300–420 mm, reconstruction matrix size=256×165, NSA=1, acquisition time=18 s;

Axial D-weighted echo planar (EPI) spin echo; single-shot, breath-hold sequence; *b* value 0–300 s/mm^2 and 0–1000 s/mm^2; TR/TE=1343/42 ms and 1867/67 ms for *b* value 0–300 s/mm^2 and 0–1000 s/mm^2, respectively; EPI factor=39; slice thickness/number=9 mm/12; intersection slice gap=1 mm; flip angle=90°; sense factor 2; FOV=300–420 mm; NSA=2; half scan factor 62%; bandwidth 1976–1493 Hz for *b* value 0–300 and 0–1000 s/mm^2, respectively; RFOV 70%; phase scan percentage 73%; acquisition voxel (mm^3) 3.32/4.55/9.00; reconstructed voxel (mm^3) 1.33/1.33/9.00; acquisition matrix 128×64; reconstruction matrix 320×220; acquisition time=17 and 22 s for *b* value 0–300 and 0–1000 s/mm^2, respectively; fat suppression obtained by spectral presaturation inversion recovery. Considering the already demonstrated liver isotropy [8], only one diffusion gradient direction was applied in every acquisition in order to reduce the minimum available TE and consequently the unwanted T_2 weighting of the Dw sequence. The orientation of the diffusion gradient is defined by the option "gradient overplus" (Philips Medical System) and the corresponding ADC maps were calculated (*b*=0–300 s/mm^2, *b*=0–1000 s/mm^2).

Moreover, a smaller cohort of 16 subjects out of 40 were submitted to a supplemental FB, multi-*b*, DwI acquisitions (16 *b* value, range 0–750 s/mm^2, with steps of 50 s/mm^2), with a total duration of 8 min and 27 s:

Axial D-weighted EPI spin echo, single-shot, TR/TE=1800/61 ms, EPI factor=39, slice thickness/number=9 mm/20, intersection gap=1 mm, flip angle=90°, sense factor 2, FOV=300–420 mm, NSA=3, half scan factor 62%, bandwidth 1976–1493 Hz, RFOV 70%, phase scan percentage 73%, acquisition voxel (mm^3) 3.32/4.55/9.00, reconstructed voxel (mm^3) 1.33/1.33/9.00, acquisition matrix 128×64, reconstruction matrix 320×220.

2.4. DwI quantitative analysis

We analyzed the middle-lower portion of the right liver lobe, where ADC values were recently demonstrated to be more repeatable and reproducible [20]. Quantitative analysis of ADC was performed with manually defined regions of interest (ROIs) (about 1250 pixels per slice for a total of 5000 pixels). We took care to include in each slice the most homogeneous portion of the middle-lower portion of the right lobe in each slice, and ROIs were placed on 4 out of 12 slices acquired, excluding four slices from the most cranial and four others from the most caudal portion of the entire liver parenchyma acquired. Furthermore, the observers took care to exclude large vessels from the ROIs (Fig. 1).

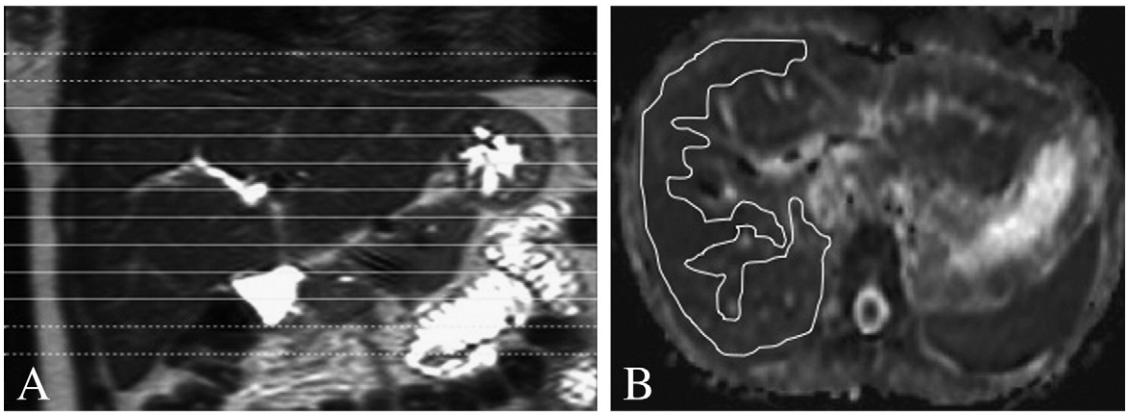

Fig. 1. ADC sampling method. (A) Four out of 12 slices acquired (broken and continuous lines) were analyzed (continuous lines) with manually defined ROIs (about 1250 pixels per slice for a total of 5000 pixels). (B) ROI sampling method: we took care to include the most homogeneous portion of the middle-lower portion of the right lobe in each slice analyzed.

Dw images were evaluated in consensus by a radiologist and a physicist (both with 4 years of experience in DwI) and then reevaluated by the study coordinator (with 12 years of experience in DwI). When the reviewers and the coordinator expressed discordant opinions about an ADC value or every other estimated parameter (>10% difference), they reached a consensus through a joint review of the images with a supplemental ADC measurement.

ADC maps calculated on BH and in vitro DwI acquisitions (b=300 and 1000 s/mm^2) were sampled using MRIcro software (1.39/5, Chris Rorden's MRIcro 1999–2005, University of South Carolina, Columbia, USA). ADC maps calculated on FB DwI acquisitions (b=50, 100, 150, 300 s/mm^2 of the multi-b acquisition) were sampled using Image J [22]. For both BH and FB acquisitions, minimum, maximum, mean ADC values, and pixel number were recorded by the two observers. Data are given for individuals and groups. ROI's data of multi-b Dw images were processed through the well-known two-compartment model of IVIM [1], based on the following equation:

$$\frac{S_b}{S_0} = (1 - \mathrm{PF})exp(-bD) + \mathrm{PF}exp(-bD^*) \quad (1)$$

where PF represents the voxel fraction of water diffusing and flowing in the random oriented capillary network, 1−PF the fraction of extravascular water random walk, D the diffusion coefficient and finally D* the pseudodiffusion coefficient, related to the mean capillary segment length and to the average blood velocity. PF, D and D* were obtained by fitting data through Eq. (1).

Since a simultaneous fit of all these parameters could be difficult, given the high dispersion and the limited sampling of DwI signals at low b value (b<150 s/mm^2) [23,24], a two-step fitting procedure was adopted, as described in other papers [25,26].

Briefly, PF and D where estimated from signal intensity data with strong diffusion weighting (b≥200 s/mm^2, where pseudodiffusion contribution is negligible) by fitting the equation

$$\frac{S_b}{S_0} = (1 - PF)exp(-bD). \quad (2)$$

In order to estimate $D*$, the outcome values of PF and D were then introduced in Eq. (1) and all multi-b (whole b range: 0–750 s/mm^2) data were subsequently processed. This two-step fitting procedure was performed using a semiautomatic homemade software driving the nonlinear regression algorithms provided in Gnuplot (http://www.gnuplot.info/, 4.4.2 release).

2.5. Statistical analysis

The mean, S.D. and 95% limits of agreement of ADC values were calculated for each group, using BH acquisitions, both at low and high b value (0–300 and 0–1000 s/mm^2, respectively); the ANOVA test was performed to evaluate differences between ADC group means. The Pearson correlation coefficient (r) was obtained to investigate the association between ADC (b values 300 and 1000 s/mm^2 for BH acquisitions and 50, 100, 150, 300 s/mm^2 for FB acquisitions), PF, D, D* and age. The variation across all ages of all these DwI parameters was assessed in a linear regression model. In case of absence of significant correlation between DwI parameters and age, the mean, S.D. and 95% limits of agreement of all the parameters were calculated considering all the subjects.

Table 1
ADC values by age group

Group	b=300 s/mm^2			b=1000 s/mm^2		
	Mean	S.D.	95% CI	Mean	S.D.	95% CI
A	2747	567	2419–3074	1650	192	1539–1761
B	2686	472	2291–3081	1483	99	1400–1565
C	2783	650	2195–3282	1555	184	1396–1714
D	2742	800	2211–3356	1558	222	1496–1620

ADC mean, S.D. and 95% confidence interval (CI) for each group both at b=300 and 1000 s/mm^2 (data in 10^{-6} mm^2/s).

Table 2
PF, *D*, *D** and ADCs of healthy subjects and correlation with age

	Method (subj. *n*)	Mean	S.D.	Mean 95% CI	*r*	*P*	*r* 95% CI
PF	FB (16)	28.57	7.40	14.07–43.07	0.30	.26	−0.23 to 0.69
D	FB (16)	1090	140	816–1364	−0.28	.30	−0.68 to 0.25
*D**	FB (16)	26728	9151	8792–44664	−0.27	.32	−0.67 to 0.26
ADC^{50}	FB (16)	3825	454	2935–4715	0.16	.67	−0.52 to 0.71
ADC^{100}	FB (16)	3333	388	2573–4093	0.39	.27	−0.32 to 0.81
ADC^{150}	FB (16)	2966	379	2223–3709	0.36	.31	−0.35 to 0.81
ADC^{300}	FB (16)	2238	251	1746–2730	0.50	.16	−0.13 to 0.87
ADC^{300}	BH (40)	2742	609	1548–3936	0.05	.74	−0.26 to 0.36
ADC^{1000}	BH (40)	1558	192	1182–1934	−0.2	.22	−0.48 to 0.08

PF (%), diffusion coefficient (*D*, in 10^{-6} mm^2/s), pseudodiffusion coefficient (*D*∗, in 10^{-6} mm^2/s), ADCs (ADC^x, in 10^{-6} mm^2/s, where *x* indicates the *b* value in s/mm^2), mean, S.D., 95% confidence interval (CI) of healthy subjects, with the corresponding Pearson correlation coefficient with age (*r*, with statistical significance, *P* and 95% CI), varying the acquisition method (FB=free-breath, BH=breath-hold) and the number of subjects.

Finally, the skewness of the distributions of 0–300 and 0–1000 s/mm^2 BH acquisition ADC values and FB acquisition *D* values was calculated considering the larger and the smaller cohort, respectively. Skewness is a measure of asymmetry of the distribution; the greater the absolute value of the skewness, the greater the asymmetry. The significance level was set at $P<.05$ for all tests. Statistical analysis was performed using SPSS (release 17.0.0, SPSS Inc., Chicago, IL, USA).

3. Results

Our scanner showed good stability, with all the *b* values adopted: repeatability and reproducibility related errors were always <1%.

For each group, mean, S.D. and 95% confidence interval of ADC values, calculated on BH with *b* value=0–300 and 0–1000 s/mm^2 Dw images, are reported (Table 1). ANOVA showed no significant differences in the mean ADC of the different groups (*P* always >.05).

No significant correlation between the subject's age and ADC was established, considering either BH or FB acquisition data, obtained at all the considered *b* values (50, 100, 150, 300, 1000 s/mm^2). The same absence of significant correlation with age was observed for PF, *D* and *D** evaluation. Pearson correlation coefficient for all the DwI parameters, with statistical significance and 95% confidence interval, is reported (Table 2). Figs. 2 and 3 show the scatterplots with linear regression line, respectively, of BH-ADC values and PF, *D*, *D** vs. age.

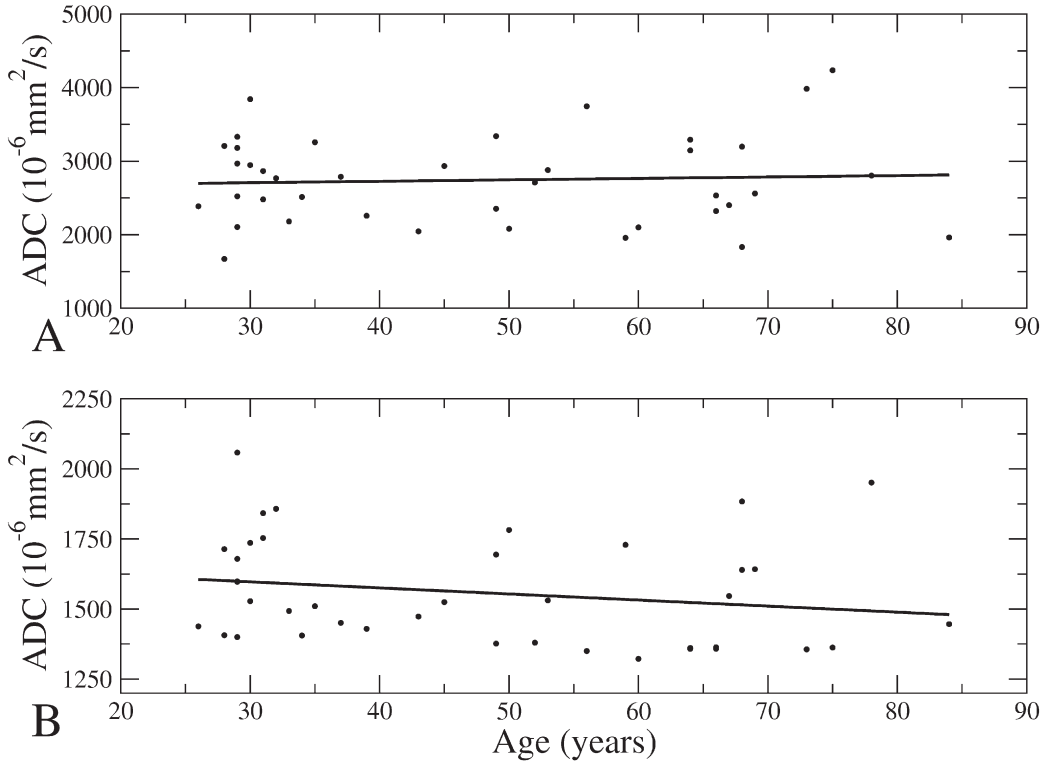

Fig. 2. Breath-hold ADC vs. age with linear regression line. Data with *b*=300 (A; upper) and *b*=1000 s/mm^2 (B; lower). The absence of a significant correlation between ADC and age, both in A and B, and the wide dispersion of data, more pronounced at *b*=300 s/mm^2 (A), should be noted.

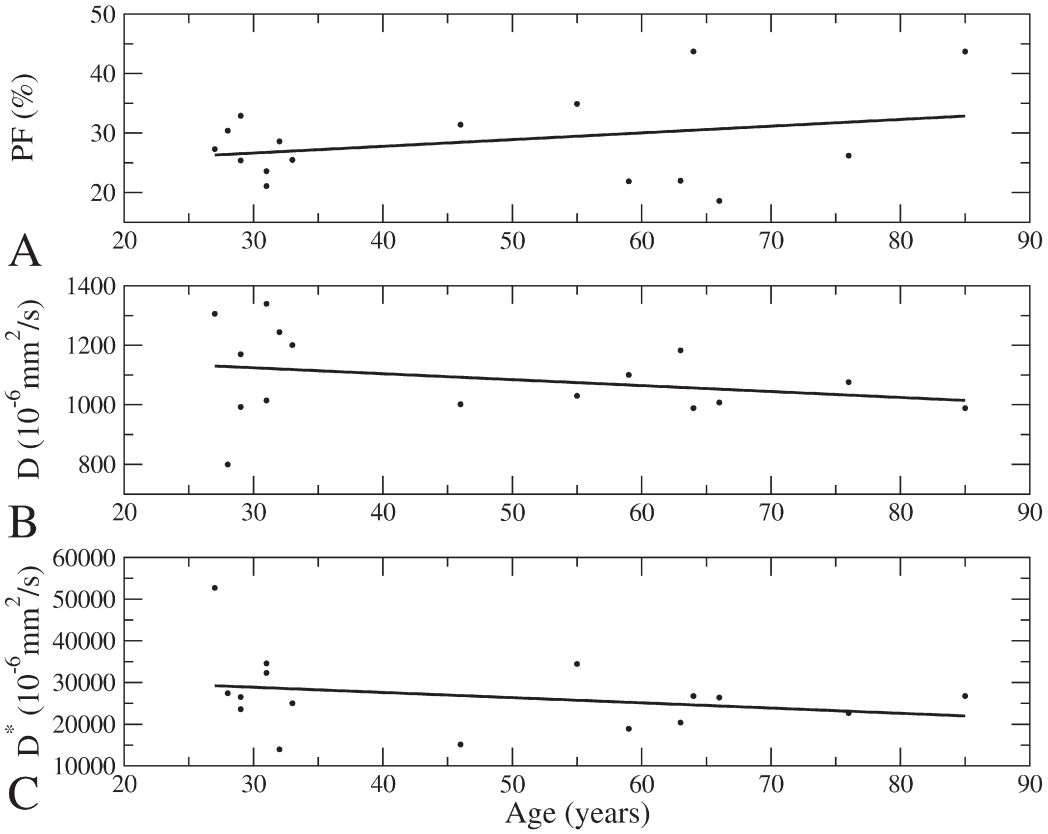

Fig. 3. PF, *D*, *D** vs. age with linear regression line. PF (A; upper), *D* (B; middle) and *D** (C; lower) values. The absence of a significant correlation between PF, *D*, *D** and age, both in A, B and C, should be noted.

Given the absence of significant correlation between all the DwI parameters and age, mean, S.D. and 95% confidence interval of each DwI parameter were calculated considering all the subjects belonging to each cohort (Table 2).

Fig. 4 shows BH-ADC histograms for all the 40 subjects at b=300 and b=1000 s/mm^2: the skewness of each distribution was 0.48 and 0.79 (b=300 and b=1000 s/mm^2, respectively).

4. Discussion and conclusion

Many efforts have been made and are ongoing to establish a correlation between DwI measurements and physiological changes in the liver where ADC measurements are frequently used to grade different levels of fibrosis [1,17,27–32]. ADC is also influenced, prevalently at low b values, by perfusion, that is strongly related to liver fibrosis and parenchymal derangement progression during chronic hepatitis [6,17,33]. The prevalent influence of perfusion has also been demonstrated in experimental animals [6]. However, as reminded in the introduction, there are many other factors, which could influence DwI quantitative measurements, and we wondered if among these, there were also the aging. Subsequently, we have firstly investigated the possible correlation between age and ADC values of the liver without finding out any significant correlation, either at low-medium b values (FB acquisitions: 50–100–150–300 s/mm^2) or medium-high b values (BH acquisitions: 300–1000 s/mm^2). This finding is unexpected since in the normal liver, aging does not imply a fibrotic/cirrhotic-like evolution [33], but it is well known that there is about a 40% reduction in blood flow and a similar or slightly less reduction in liver mass [33–39]. The reasons for this age-linked reduction in hepatic blood flow and volume, which are perhaps related, are still unknown but perplexing since there seem to be few significant structural or biochemical changes in the aging liver [40–42]. With a relevant decrement of liver blood flow, one would presume that there would be a decrease in ADC values with age, at least at lower b values. In our series, the width and asymmetry of ADC histogram not only show that the ADC values are affected by a perfusion phenomenon, but also that its spread is probably due to different components of flow and to a large variability in PFs. This probably also reflects the observed change in skewness between b=300 and b=1000 s/mm^2 ADC distributions and the symmetry of the D values distribution (0.48, 0.79 and 0.06, respectively). In fact, at high b value, the diffusion component is predominant in ADC measurements and the residual effect of perfusion probably contributes to the asymmetric right tail of the ADC histogram (Fig. 4): the absence of asymmetry in the D value distribution supports this hypothesis. This ADC stability during different ages offers

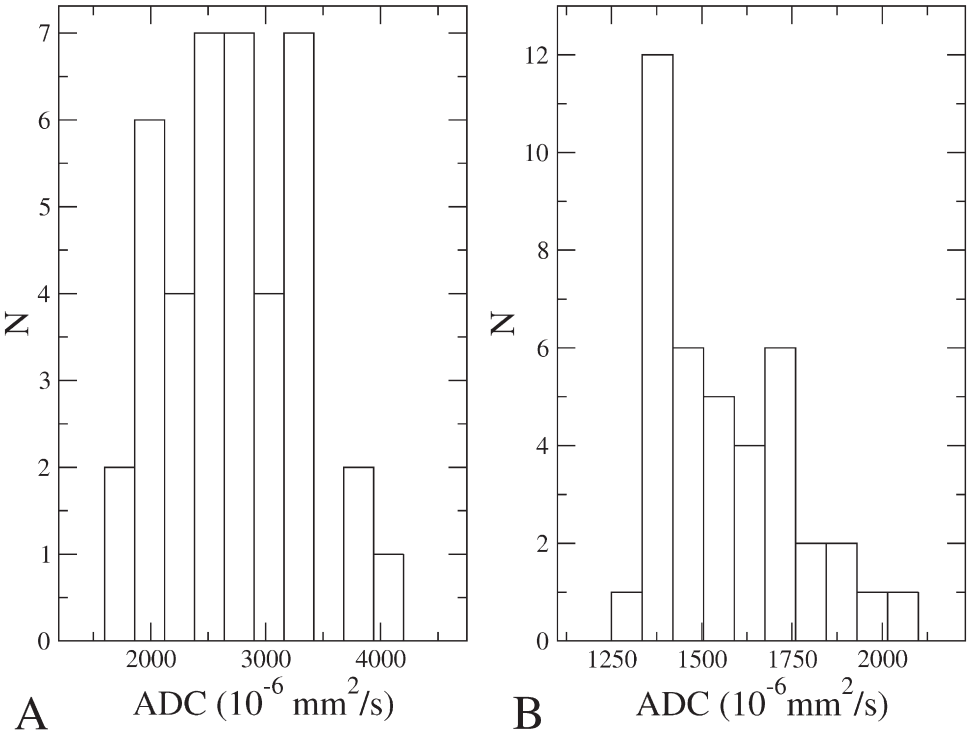

Fig. 4. Histogram of breath-hold ADC values. Data at b=300 (bin size=260×10^{-6} mm^2/s) (A; left) and b=1000 s/mm^2 (bin size=85×10^{-6} mm^2/s) (B; right). The higher ADC mean value at b=300 s/mm^2 (A) compared to b=1000 s/mm^2 (B) and the more symmetric shape of ADC distribution in (A) vs. (B) (skewness=0.48 and 0.79, respectively) should be noted.

the possibility to use, in the future, non-age-matched groups in studies on liver ADC. Moreover, ADC variation that has already been observed and reported in the literature cannot be ascribed to ADC age-related changes: this is important especially in diffuse liver disease studies, which usually involve older patients. Furthermore, the documented wide range of liver parenchyma ADC values (at b=1000 s/mm^2) among healthy subjects, from around 1300 to 2000×10^{-6} mm^2/s (Fig. 2), suggests that it is improbable that this technique provides a valid mean value as a reference for all or at least most of the subjects. We can argue that quantitative DwI seems more useful in following a single subject's disease over time and is therefore more appropriate for longitudinal rather than cross-sectional studies. In fact, recent literature reports have shown that ADC is not satisfactory for distinguishing different solid focal liver lesions [27,28,43] or grading fibrosis [3–5,44]. On the contrary, results of the studies devoted to the evaluation and follow-up of the response of metastatic liver tumors to chemotherapy are hopeful [42,44,45].

To better investigate possible age-related quantitative DwI variations, we examined also PF, D and D* in a smaller cohort of 16 volunteers (four for each age group), using a multi-b sequence with many D weightings, which allows an highly accurate representation of DwI signal decay. Interestingly, we did not find any significant correlation also with these non-b-linked parameters and age, even if a nonsignificant increase of PF and decrease of D and D* were observed.

The slight decrease in D value with aging (Table 2) could find a partial explanation in studies which have reported that there are significant age-associated reductions in the fenestration of liver sinusoidal endothelial cells in rats; increased expression of von Willebrand's factor; and increased deposition of extracellular matrix, basal lamina and connective tissue elements in the space of Disse [46]. Conversely, on the basis of 40% reduction in blood flow, a significant difference with aging can be expected in flow-related DwI parameters.

Expressing PF, the fraction of water molecules in the capillary network (blood) within the voxel, it is possible that this parameter is insensitive to perfusion changes in liver aging because in this case, flow and volume equally decrease. Instead, D* is related to the net capillary flow within the voxel, and then it seems to be a suitable parameter to study flow variation. Though, considering that the estimation of D* is strongly dependent on the lower b value data, where the standard error is really relevant, it is possible that flow variation with age might be hidden by the wide dispersion of data (about ±35%, Table 2).

The first limitation of our study is represented by the small-sized cohort submitted to the multi-b sequence. However, the size of our control group is comparable with those reported in other recent papers [4,8,23] and allows us to show at least a preliminary trend. Secondly, in our scanner, echo-navigator technique is not available, and then we have obtained multi-b sequence in FB modality, surely

less reproducible than that acquired with navigator. Nevertheless, our results seem to be reliable considering the slightly dissimilar ADC values with differences that can be easily explained by the diverse acquisition modalities at b=300 s/mm^2 (BH and FB) and TE (42 and 61 ms for BH and FB, respectively). Moreover, the use of echo-navigator would increase significantly the already relevant acquisition time (8 min and 27 s), reducing the feasibility of the multi-b sequence (16 in our experience) in clinical practice.

In conclusion, our study on healthy liver parenchyma indicates that there are no significant variations in liver DwI quantitative parameters (ADC, PF, D, and D*) according to the age of the subject.

References

[1] Le Bihan D, Breton E, Lallemand D, Grenier P, Cabanis E, Laval JM. Separation of diffusion and perfusion in intravoxel incoherent motion MR imaging. Radiology 1988;168:497–505.

[2] Colagrande S, Pallotta S, Vanzulli A, Napolitano M, Villari N. The diffusion parameter in magnetic resonance: physics, techniques and semeiotics. Radiol Med 2005;109:1–16.

[3] Naganawa S, Kawai H, Fukatsu H, Sakurai Y, Aoki I, Mimiura S, et al. Diffusion-weighted imaging of the liver: technical challenges and prospects for the future. Magn Reson Med Sci 2005;4:175–86.

[4] Taouli B, Tolia AJ, Losada M, Babb JS, Chan SE, Bannan MA, et al. Diffusion-weighted MRI for quantification of liver fibrosis: preliminary experience. Am J Roentgenol 2007;189:799–806.

[5] Girometti R, Furlan A, Esposito G, Bazzocchi M, Como G, Soldano F, et al. Relevance of b-values in evaluating liver fibrosis: a study in healthy and cirrhotic subjects using two single-shot spin-echo echo-planar diffusion-weighted sequences. J Magn Reson Imaging 2008;28: 411–9.

[6] Annet L, Peeters F, Abarca-Quinones J, Leclercq I, Moulin P, Van Beers BE. Assessment of diffusion-weighted MR imaging in liver fibrosis. J Magn Reson Imaging 2007;25:122–8.

[7] Girometti R, Furlan A, Bazzocchi M, Soldano F, Isola M, Bitetto D, et al. Diffusion-weighted MRI in evaluating advanced liver fibrosis in cirrhotic patients: a study of feasibility. Radiol Med 2007;112:394–408.

[8] Taouli B, Vilgrain VR, Dumont E, Daire JL, Fan B, Menu Y. Evaluation of liver diffusion isotropy and characterization of focal hepatic lesions with two single-shot echo-planar MR imaging sequences: prospective study in 66 patients. Radiology 2003;226:71–8.

[9] Taouli B, Sandberg A, Stemmer A, Parikh T, Wong S, Xu J, et al. Diffusion-weighted imaging of the liver: comparison of navigator triggered and BH acquisitions. J Magn Reson Imaging 2009;30:561–8.

[10] Kwee TC, Takahara T, Koh DM, Nievelstein RA, Luijten PR. Comparison and reproducibility of ADC measurements in breath-hold, respiratory triggered, and free-breathing diffusion-weighted MR imaging of the liver. J Magn Reson Imaging 2008;28:1141–8.

[11] Kandpal H, Sharma R, Madhusudhan KS, Kapoor KS. Respiratory-triggered versus breath-hold diffusion-weighted MRI of the liver lesions: comparison of image quality and apparent diffusion coefficient values. AJR Am J Roentgenol 2009;192:915–22.

[12] Schraml C, Nina FS, Clasen S. Navigator respiratory-triggered diffusion-weighted imaging in the follow-up after hepatic radio-frequency ablation-initial results. J Magn Reson Imaging 2009;29: 1308–16.

[13] Braithwaite AC, Dale BM, Boll DT, Merkle EM. Short- and mid-term reproducibility of apparent diffusion coefficient measurements at 3.0-T diffusion-weighted imaging of the abdomen. Radiology 2009;250: 459–65.

[14] Conturo TE, McKinstry RC, Aronovitz JA, Neil JJ. Diffusion MRI: precision, accuracy and flow effects. NMR Biomed 1995;8:307–32.

[15] Colagrande S, Belli G, Politi LS, Mannelli L, Pasquinelli F, Villari N. The influence of diffusion and relaxation-related factors on signal intensity: an introductive guide to magnetic resonance diffusion-weighted imaging studies. J Comput Assist Tomogr 2008;32:463–74.

[16] Kwee TC, Takahara T, Niwa T, Ivancevic MK, Herigault G, Van Cauteren M, et al. Influence of cardiac motion on diffusion-weighted magnetic resonance imaging of the liver. Magn Reson Mater Phys 2009;22:319–25.

[17] Le Bihan D. Intavoxel incoherent motion perfusion MR imaging: a wake up call. Radiology 2008;249:748–52.

[18] Murtz P, Flacke S, Traber F, van den Brink JS, Gieseke J, Schild HH. Abdomen: diffusion-weighted MR imaging with pulse-triggered single-shot sequences. Radiology 2002;224:258–64.

[19] Padhani AR, Liu G, Mu-Koh D, et al. Diffusion-weighted magnetic resonance imaging as a cancer biomarker: consensus and recommendations. Neoplasia 2009;11:102–25.

[20] Colagrande S, Pasquinelli F, Mazzoni LN, Belli G, Virgili G. MR-diffusion weighted imaging of healthy liver parenchyma: repeatability and reproducibility of apparent diffusion coefficient measurement. J Magn Reson Imaging 2010;31:912–20.

[21] Lee SW, Park SH, Kim KW. Unenhanced CT for assessment of macrovesicular hepatic steatosis in living liver donors: comparison of visual grading with liver attenuation index. Radiology 2007;244: 479–85.

[22] Abramoff MD, Magelhaes PJ, Ram SJ. Image processing with ImageJ. Biophotonics Int 2004;7:36–42.

[23] Patel J, Sigmund EE, Rusinek H, Oei M, babb JS, Taouli B. Diagnosis of cirrhosis with intravoxel incoherent motion diffusion MRI and dynamic contrast-enhanced MRI alone and in combination: preliminary experience. J Magn Reson Imaging 2010;31:589–600.

[24] Istratov AA, Vyvenko OF. Exponential analysis in physical phenomena. Rev Sci Instrum 1999;70:1233–57.

[25] Callot V, Bennett E, Decking UK, Balaban RS, Wen H. In vivo study of microcirculation in canine myocardium using the IVIM method. Magn Reson Med 2003;50:531–40.

[26] Wirestam R, Borg M, Brockstedt S, Lindgren A, Holtas S, Stahlberg F. Perfusion-related parameters in intravoxel incoherent motion MR imaging compared with CBV and CBF measured by dynamic susceptibility-contrast MR technique. Acta Radiol 2001;42:123–8.

[27] Sandrasegaran K, Akisik FM, Lin C, Tahir B, Rajan J, Aisen AM. The value of diffusion-weighted imaging in characterizing focal liver masses. Acad Radiol 2009;16:1208–14.

[28] Parikh T, Drew SJ, Lee VS, Wong S, Hecht EM, babb JS, Taouli B. Focal liver lesion detection and characterization with diffusion-weighted MR imaging: comparison with standard breath-hold T2-weighted imaging. Radiology 2008;246:812–22.

[29] Muller MF, Prasad P, Siewert B, Nissenbaum MA, Raptopoulos V, Edelman RR. Abdominal diffusion mapping with use of a whole body echo-planar system. Radiology 1994;190:475–8.

[30] Tha KK, Terae S, Yabe I, Miyamoto T, Soma H, Zaitsu Y, et al. Microstructural white matter abnormalities of multiple system atrophy: in vivo topographic illustration by using diffusion-tensor MR imaging. Radiology 2010;255:563–9.

[31] Langer DL, van der Kwast TH, Evans AJ, Plotkin A, Trachtenberg J, Wilson BC, et al. Prostate tissue composition and MR measurements: investigating the relationships between ADC, T2, K(trans), v(e), and corresponding histologic features. Radiology 2010;255:485–94.

[32] Luciani A, Vignaud A, Cavet M, Van Nhieu JT, Mallat A, Ruel L, et al. Liver cirrhosis: intravoxel incoherent motion MR imaging-pilot study. Radiology 2008;249:748–52.

[33] Schmucker DL. Age-related changes in liver structure and function: implications for disease? Exp Gerontol 2005;40:650–9.

[34] Le Couteur DG, McLean AJ. The aging liver: drug clearance and an oxygen diffusion barrier hypothesis. Clin Pharmacokinetics 1998;34: 359–73.

[35] McLlean AJ, Le Couter DG. Aging biology and geriatric clinical pharmacology. Pharmacol Rev 2004;56:163–84.

[36] Wynne HA, Cope LH, James OF, Rawlins MD, Woodhouse KW. The effect of age and frailty upon acetanilide clearance in man. Age Ageing 1989;18:415–8.
[37] Iber FL, Murphy PA, Connor ES. Age-related changes in the gastrointestinal system. Effects on drug therapy. Drugs Aging 1994;5:34–48.
[38] Zeek J, Paltt D. Age related changes in the liver. Consequences for drug therapy. Fortschr Med 1990;30:651–3.
[39] Ito Y, Sørensen KK, Bethea NW, Svistounov D, McCuskey MK, Smedsrød BH, et al. Age-related changes in the hepatic microcirculation in mice. Exp Gerontol 2007;42:789–97.
[40] Jansen PL. Liver disease in the elderly. Best Pract Res Clin Gastroenterol 2002;16:149–58.
[41] Popper H. Aging and the liver. Prog Liver Dis 1986;8:659–83.
[42] Cui Y, Zhang XP, Sun YS, Tang L, Shen L. Apparent diffusion coefficient: potential imaging biomarker for prediction and early detection of response to chemotherapy in hepatic metastases. Radiology 2008; 248:894–900.
[43] Holzapfel K, Bruegel M, Eiber M, et al. Characterization of small ($b \leq 10$ mm) focal liver lesions: value of respiratory-triggered echo-planar diffusion-weighted MR imaging. Eur J Radiol 2010;76:89–95.
[44] Talwalkar JA, Yin M, Fidler JL, Sanderson SO, Kamath PS, Ehman RL. Magnetic resonance imaging of hepatic fibrosis: emerging clinical applications. Hepatology 2008;47:332–42.
[45] Marugami N, Tanaka T, Kitano S, Hirohashi S, Nishiofuku H, Takahashi A, et al. Early detection of therapeutic response to hepatic arterial infusion chemotherapy of liver metastases from colorectal cancer using diffusion-weighted MR imaging. Cardiovasc Intervent Radiol 2009;32:638–46.
[46] Le Couteur DG, Fraser R, Cogger VC, McLean AJ. Hepatic pseudocapillarisation and atherosclerosis in ageing. Lancet 2002;35:1612–5.